Journal of Civil Engineering and Urban Planning (2026)
Clausius Scientific Press, Canada

DOI: 10.23977/jceup.2026.080110
ISSN 2616-3969 Vol. 8 Num. 1

Intelligent Displacement Back Analysis and Reinforcement Calculation Method for Rock Slopes Based on Intelligent Computation

Huijing Duan, Gongxing Yan*, Peng Liu

School of Intelligent Construction, Luzhou Vocational and Technical College, Luzhou, 646000, Sichuan, China
**Corresponding author*

Keywords: Rock slope stability analysis; displacement inverse analysis; intelligent optimization algorithm; numerical calculation model; reinforcement optimization design

Abstract: As the scope of rock slope engineering grows and the complexity of the service environment increases, the traditional stability assessment methods based on empirical parameters and single numerical analysis cannot reflect the actual mechanical response of slopes, and thus, issues like wide parameter uncertainties, low predictive accuracy of displacement, and dependence on experience in the design of reinforcements are found. To overcome these weaknesses, this paper proposes an intelligent calculation approach to build a combined calculation approach to the back analysis of the slope displacement of rocks and the optimization of reinforcement based on monitoring data. Regarding the method implementation, an error minimization model of measured and calculated displacements is created, and a particle swarm optimization algorithm is applied to invert the major parameters, including elastic modulus, cohesion and internal friction angle. According to this, the inverted parameters are incorporated into a numerical model and the displacement and stress fields are coupledly calculated, and the possible slip modes are determined using the indices of displacement gradient and shear strain. Moreover, a multi-objective optimization model with the displacement control and the stability improvement as its objectives are developed in order to logically reverse engineer the reinforcement parameters like anchor length, spacing and prestress and, in this way, attain optimized design of the reinforcement scheme. The research shows that the approach can be effective in enhancing the parameter identification accuracy and rationality of reinforcement design to give a data-driven intelligent calculation path of the analysis of the stability and engineering of the reinforcements of rock slopes.

1. Introduction

As the construction of large-scale infrastructure continues to develop, the use of rock slopes in transportation and water conservancy and mining engineering becomes more and more common. They are directly connected to engineering safety and reliability in their operations [1-2]. The effects of the complex geological conditions and the multi-field coupling effects cause the slope

mechanical parameters to have serious uncertainties and spatial variability, so the traditional methods that use empirical values and one numeric analysis are not accurate in their reflection of the actual deformation and failure properties. In addition, the current stability approaches are mostly associated with fixed parameter input without proper use of monitoring data and dynamic determination of slope conditions [3]. In reinforcement design, engineering practice still primarily relies on empirical methods and trial calculations, resulting in problems such as blind parameter selection, low design efficiency, and insufficient optimization. Therefore, how to utilize measured data to improve parameter identification accuracy and achieve intelligent and quantitative slope analysis and reinforcement design has become a key bottleneck in current research.

To address these issues, this paper proposes a method for displacement back analysis and reinforcement optimization calculation of rock slopes based on intelligent computing. First, an inverse analysis model constrained by measured displacement is constructed, and an intelligent optimization algorithm is introduced to achieve high-precision inversion of key mechanical parameters of the rock mass. Based on this, a numerical calculation model driven by the inversion parameters is established to perform coupled analysis of the slope displacement and stress fields, and potential slip modes are identified by combining displacement gradient and shear strain indices. Furthermore, a reinforcement parameter optimization model aimed at displacement control and stability improvement is constructed, intelligently inversely calculating key design parameters such as anchor bolts to achieve optimized configuration of reinforcement schemes. The proposed method is validated through typical engineering examples. The results show that this method can effectively improve the accuracy of displacement prediction and the rationality of reinforcement design, providing a data-driven technical approach for the stability analysis and engineering treatment of rock slopes.

2. Related Works

The stability of rock slopes has been studied in various aspects in the available literature such as in the context of monitoring and identification, numerical simulation, mechanism analysis and engineering protection, and has over the years shifted its focus on single analysis to multi-method integration. Long-term monitoring of the evolution of landslide deformation was performed by Kuo et al., on the basis of optical satellite images, indicating that the velocity and acceleration of the landslide were growing significantly prior to instability and showing its strong dependence on rainfall. Meanwhile, they suggested an instability criterion on the basis of velocity-acceleration threshold, which offers a valuable concept of early warning of slope instability [4]. Based on this fact, Amagu et al. integrated on-site multi-point displacement measurements and three-dimensional finite element numerical modeling, inverted rock mechanics parameters using an inversion analysis and elastoplastic model to simulate and confirm slope deformation, enhancing the accuracy and reliability of the stability assessment [5]. In comparison with the simple monitoring or simulation studies, Zhang et al. began with the macroscopic geological structure and employed a discrete fracture network model to expose the drawer-type sliding failure mechanism of steeply dipping bedding slopes under the influence of faults and joints, where structural planes are the most important factors in controlling the slope instability [6]. Experimentally, Zhao et al. examined the toppling deformation behavior of reverse-dip layered rock slopes in terms of physical model tests, indicating that the various slopes have varying failure modes under varying lithological conditions, and a grading method is offered on basis of rock layer flip angle angle, which offers a quantitative framework of deformation recognition [7]. To understand the evolution of the instability process of high mine slopes, Tao et al. adopted the combination of physical models and numerical simulations and divided the process into stages to explore the path of the evolution of the instability process,

beginning with the crack initiation and culminating in through-instability, which was a process-based understanding of disaster prevention and control [8]. In engineering protection, Maheshwari studied the impact resistance of reinforced protective dikes based on trajectory analysis and finite element method for rockfall risk, showing that reinforced structures can effectively improve energy dissipation capacity and structural stability [9]. Overall, although existing research has made some progress in monitoring and identification, mechanism analysis and protection design, the methods are still relatively fragmented, especially in the integration of "monitoring data - parameter inversion - stability analysis - reinforcement optimization", there is still room for improvement.

3. Methods

3.1 Displacement Back Analysis Method for Rock Slopes

3.1.1 Data-Driven Parametric Inversion Model

Using displacement data acquired by the slope monitoring system as constraints, and the finite element method or numerical calculation model as the forward analysis tool, a mapping relationship between the parameter vector and the displacement response is established. Let the measured displacement be (u_i^{obs}), and the calculated displacement be $(u_i^{cal}(\theta))$, where (θ) represents the set of parameters to be inverted (such as elastic modulus, cohesion, and internal friction angle, etc.). Then, the following objective function can be constructed:

$$F(\theta)=\sum_{i=1}^{n} w_i \left(u_i^{obs}-u_i^{cal}(\theta)\right)^2 \tag{1}$$

Among them, (w_i) is the weighting coefficient, used to reflect the importance or reliability of data from different monitoring points. By minimizing the objective function, the calculated displacement approximates the measured displacement, thereby deriving mechanical parameters that better reflect the actual working conditions.

During model construction, to improve the stability and engineering applicability of the inversion results, regularization constraints or parameter boundary conditions can be further introduced to avoid non-physical parameter values. Simultaneously, a time-series inverse analysis model can be constructed by combining multi-time monitoring data, enabling the parameter identification results to reflect the dynamic characteristics of the slope deformation evolution process.

3.1.2 Intelligent Optimization Algorithm for Inverse Analysis Solution

Since inverse analysis problems typically exhibit high-dimensional nonlinearity and multi-peak characteristics, traditional gradient-based optimization methods are prone to getting trapped in local optima, making it difficult to obtain stable and reliable parameter solutions. Therefore, an intelligent optimization algorithm is introduced to perform a global search on the inverse analysis model to improve the accuracy and efficiency of parameter inversion.

Taking the Particle Swarm Optimization (PSO) algorithm as an example, the parameter vector (θ) to be inverted is considered as the position of a particle, and the search is performed in a (D)-dimensional parameter space. In the (k)th iteration, the velocity and position update formulas for the (i)th particle are:

$$v_i^{k+1}=\omega v_i^k+c_1 r_1 \left(p_i^k-x_i^k\right)+c_2 r_2 \left(g^k-x_i^k\right) \tag{2}$$

$$x_i^{k+1}=x_i^k+v_i^{k+1} \tag{3}$$

Among them, (x_i^k) represents the position (i)th particle in the (k)th iteration (i.e., the parameter value), (v_i^k) is its velocity; (p_i^k) is the individual's historical best position, (g^k) is the group's global best position; (ω) is the inertia weight, (c_1) and (c_2) are learning factors, and (r_1) and (r_2) are random numbers in the interval ([0,1]).

In each iteration, the parameters corresponding to the current position of the particle are input into the numerical calculation model to obtain the calculated displacement $(u_i^{cal}(\theta))$, which is then substituted into the objective function:

$$F(\theta)=\sum_{j=1}^{n} w_j \left(u_j^{obs}-u_j^{cal}(\theta)\right)^2 \tag{4}$$

The parameters are gradually optimized by comparing the objective function value with the individual optimal solution and the global optimal solution.

To avoid premature convergence of the algorithm, an adaptive inertia weight strategy can be adopted:

$$\omega=\omega_{max}-\frac{k}{k_{max}}(\omega_{max}-\omega_{min}) \tag{5}$$

Among them, (k_{max}) is the maximum number of iterations, and (ω_{max}) and (ω_{min}) are the upper and lower limits of the inertia weight, respectively. This strategy enhances the global search capability in the early stage and improves the local convergence accuracy in the later stage.

In addition, to further improve the stability of the solution, boundary constraints can be introduced in the parameter update process:

$$\theta_j^{min}\le\theta_j\le\theta_j^{max} \tag{6}$$

This ensures that the inversion parameters have reasonable physical meaning.

3.2 Displacement Response Calculation and Stability Identification Methods

3.2.1 Numerical Calculation Model Driven by Inversion Parameters

During the calculation process, the constitutive relation of the rock mass can be expressed as:

$$\sigma=D(\theta)\varepsilon \tag{7}$$

Among them, (σ) is the stress tensor, (ε) is the strain tensor, and $(\mathbf{D}(\theta))$ is the constitutive matrix determined by the inversion parameter (θ). By inputting the elastic modulus, Poisson's ratio, and strength parameters obtained from the inversion analysis into the constitutive model, the authenticity and reliability of the calculation results can be significantly improved.

Furthermore, a system of governing equations is established based on the equilibrium equations and geometric equations:

$$\nabla\cdot\sigma+b=0 \tag{8}$$

$$\varepsilon=\frac{1}{2}(\nabla u+\nabla u^T) \tag{9}$$

Among them, $(\boldsymbol{u})$ is the displacement vector, and $(\boldsymbol{b})$ is the body force term. By discretizing and solving the above equation system, the displacement and stress distribution of each node inside the slope can be obtained.

It is assumed that the shear strength parameters satisfy:

$$c'=\frac{c}{F_s},\quad \tan\varphi'=\frac{\tan\varphi}{F_s} \tag{10}$$

Among them, (F_s) is the safety factor. When the calculation model reaches the limit equilibrium state, the corresponding (F_s) is the slope stability safety factor.

3.2.2 Deformation Feature Extraction and Slip Pattern Recognition

First, by calculating the displacement gradient tensor:

$$\nabla u=\begin{bmatrix}\frac{\partial u}{\partial x} & \frac{\partial u}{\partial y}\\ \frac{\partial v}{\partial x} & \frac{\partial v}{\partial y}\end{bmatrix} \tag{11}$$

The non-uniform distribution characteristics of the slope's internal deformation can be obtained. When the displacement gradient in a certain area increases significantly, it usually corresponds to a potential slip zone or a concentrated shear deformation area.

Furthermore, the shear strain index is introduced to quantify the degree of deformation concentration:

$$\gamma=\sqrt{\left(\frac{\partial u}{\partial y}+\frac{\partial v}{\partial x}\right)^2} \tag{12}$$

When the shear strain (γ) exceeds a certain threshold, the area can be determined as a potential failure zone, thereby identifying the location and development trend of the slip surface.

In addition, the displacement mutation criterion can be used for auxiliary judgment:

$$\Delta u=\left|u_{i+1}-u_i\right| \tag{13}$$

When there is a significant change in the displacement difference between adjacent nodes, it indicates that there may be a structural discontinuity or slip interface in the region.

3.3 Optimization Calculation Method for Rock Slope Reinforcement

3.3.1 Parametric Representation and Calculation Model for Reinforcement

To achieve computability and intelligent optimization of slope reinforcement design, it is necessary to uniformly parametrically represent various reinforcement measures. For common structural forms such as anchor bolts and anti-slide piles, their key design variables are abstracted into parameter vectors:

$$x=L,s,\alpha,T,d,h,n \tag{14}$$

Among them, (L) is the anchorage length, (s) is the spacing, (α) is the inclination angle, (T) is the prestress, (d) and (h) are the diameter and burial depth of the anti-slide piles, respectively, and (n) is the number of piles. Through the above parametric representation, the discrete engineering design problem can be transformed into a continuous optimization problem.

In numerical calculation, the influence of the reinforcement structure on slope stability is mainly reflected in two aspects: additional resistance and deformation constraints. Taking the anchor rod as an example, its anti-sliding contribution can be expressed as:

$$R_a=\sum_{i=1}^{n} T_i\cos\alpha_i \tag{15}$$

Among them, (T_i) is the axial force of the (i)th anchor rod, and (α_i) is its inclination angle. The resistance of the anti-sliding pile can be calculated through the pile-soil interaction model, and its

total anti-sliding force can be approximately expressed as:

$$R_p=\sum_{j=1}^{m}\left(k_s\cdot\delta_j\cdot A_j\right) \tag{16}$$

Among them, (k_s) is the foundation reaction coefficient, (δ_j) is the pile displacement, and (A_j) is the area of action.

After embedding the reinforced structure parameters into the numerical model, a mapping relationship between "reinforcement parameters - displacement response - stability index" can be established:

$$u=f(\theta,x) \tag{17}$$

$$F_s=g(\theta,x) \tag{18}$$

Among them, (θ) is the rock mass parameter obtained by inversion, $(\boldsymbol{x})$ is the reinforcement parameter, $(\boldsymbol{u})$ is the displacement response, and (F_s) is the safety factor. This model provides a basis for subsequent optimization calculations.

3.3.2 Optimization of Reinforcement Parameters Based on Intelligent Algorithms

In the reinforcement design process, a multi-objective optimization model is constructed with the goal of controlling slope displacement or improving the stability safety factor, to achieve the inverse calculation and optimal configuration of reinforcement parameters.

First, the optimization objective function is defined. When displacement control is the objective, the following objective function can be constructed:

$$\min ; F_1(x)=\sum_{i=1}^{n} w_i \left|u_i(x)\right| \tag{19}$$

When stability improvement is the objective, the following can be defined:

$$\max ; F_2(x)=F_s(x) \tag{20}$$

Furthermore, a comprehensive multi-objective optimization model can be constructed:

$$\min ; F(x)=\lambda_1 F_1(x)-\lambda_2 F_2(x) \tag{21}$$

Among them, (λ_1) and (λ_2) are weighting coefficients used to balance the relationship between displacement control and stability improvement.

Meanwhile, to ensure that the optimization results meet the actual requirements of the project, the following constraints are introduced:

$$\begin{cases}\theta_j^{\min}\le x_j\le\theta_j^{\max}\\ F_s(x)\ge F_s^{req}\\ u_i(x)\le u^{allow}\end{cases} \tag{22}$$

Among them, (F_s^{req}) is the minimum safety factor required by the specification, and (u^{allow}) is the allowable displacement value.

In the solution process, intelligent optimization algorithms (such as particle swarm optimization or genetic algorithm) are introduced to solve the above model. Taking the particle swarm optimization algorithm as an example, the reinforcement parameter vector $(\boldsymbol{x})$ is used as the particle position, and the global search is achieved through velocity and position updates:

$$v_i^{k+1}=\omega v_i^k+c_1 r_1(p_i^k-x_i^k)+c_2 r_2(g^k-x_i^k) \tag{23}$$

$$x_i^{k+1}=x_i^k+v_i^{k+1} \tag{24}$$

4. Results and Discussion

4.1 Engineering Examples and Data Sources

A typical rock slope project is selected as the research object. The slope has a layered structure as a whole, with local structural surfaces. The monitoring system deploys multiple sets of displacement monitoring points to acquire horizontal and vertical displacement data at different time periods, forming a continuous time series dataset. To ensure data validity, outlier removal and smoothing are performed on the original monitoring data, and a unified coordinate benchmark is established.

4.2 Back Analysis Calculation Settings

In the back analysis process, elastic modulus, cohesion, and internal friction angle are selected as the parameters to be inverted, and their initial search ranges are set as shown in Table 1.

Table 1. Inversion Parameters

Parameter	Lower Bound	Upper Bound
Elastic Modulus E (MPa)	500	5000
Cohesion c (kPa)	20	200
Internal Friction Angle φ (°)	20	45

The parameter search was done using a smart optimization algorithm with the settings of the number of particles, the maximum number of iterations, and the convergence threshold. In the back analysis, monitoring points displacement error was taken as the evaluation index, and the optimal parameter combination was calculated after several iterations. In order to prevent the effect of randomness, the back analysis process was independently repeated several times and a mean value of the result was taken as the final inversion parameters.

4.3 Displacement Response Calculation and Stability Analysis Setup

According to the parameters obtained when inverting the parameters, a numerical calculation model of the slope was developed to solve the displacement and stress fields. In the calculation, the displacement response of the key monitoring points was measured and the general deformation characteristics were obtained.

The stability test was done using strength reduction approach whereby the safety factor was determined by successively reducing the shear strength parameter. In the calculation, the development process of the slope deformation was recorded, and the shear strain distribution was taken to determine the possible slip zones.

At the same time, the indicators that were to be analyzed further were taken out and included:

Peak displacement, and its position;

Displacement gradient distribution characteristics;

Shear strain concentration zone range;

Trend of change in safety factors.

4.4 Reinforcement Optimization Calculation Settings

The key optimization variables used in the reinforcement calculation were the length of the anchor, the spacing, and the prestress, the ranges of these variables were chosen:

Table 2. Optimization Variables

Parameter	Lower Bound	Upper Bound
Bolt Length L (m)	5	20
Bolt Spacing s (m)	1	4
Prestress T (kN)	50	300

A space of parameter combinations of the reinforcement schemes was built, and intelligent search was carried out with the help of intelligent optimization algorithm. A numerical model was used to compute and analyze the displacement and safety factor of each combination of parameters (see Table 2).

In order to optimize the efficiency of the screening mechanism, a constraint screening mechanism was proposed to discard schemes, which do not satisfy the stability requirements earlier, hence minimizing the number of invalid calculations.

4.5 Evaluation Indicators and Result Comparison Methods

To quantitatively evaluate the effectiveness of the method, the following evaluation indicators were selected:

(1) Displacement Error Index

Used to evaluate the accuracy of the back analysis:

$$RMSE=\sqrt{\frac{1}{n}\sum_{i=1}^{n}\left(u_i^{obs}-u_i^{cal}\right)^2} \tag{25}$$

(2) Displacement Control Rate

Used to measure the reinforcement effect:

$$\eta=\frac{u_{before}-u_{after}}{u_{before}}\times 100\% \tag{26}$$

(3) Stability Improvement Coefficient

$$\Delta F_s=F_s^{after}-F_s^{before} \tag{27}$$

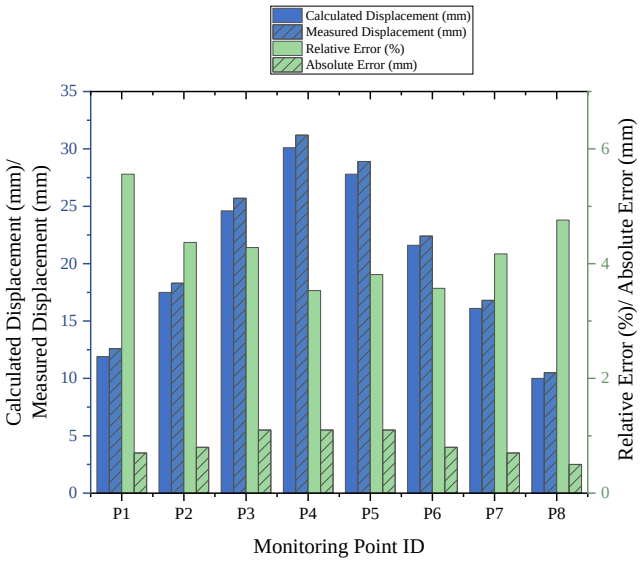

Figure 1. Comparison of Back Analysis Results and Measured Displacement

Note: Monitoring points were laid out along the slope surface and numbered sequentially from the top to the bottom of the slope.

The results of the back-analysis calculation (see Figure 1) are usually in good agreement with the measured displacements. The comparative errors of every monitoring point are all managed within the band of 3.53% to 5.56% and this is an indication that the developed parameter inversion model can effectively represent the real deformation behavior of the rock slope. The value of the displacement at the monitoring points in the middle of the slope (P3–P5) is greater spatially, which is associated with slightly greater but constant calculation errors, which means that the model remains well adapted to high-deformation areas. The top (P1) and toe (P8) displacement on slope are smaller and there is a slight variation in the error levels, however, in general the error levels do not vary significantly. The error values exceeding the 1.1 mm are all less than the error value which shows the high precision of the back-analysis results.

Table 3. Comparison of Slope Response before and after Reinforcement Optimization

Indicator	Before Reinforcement	After Reinforcement (Optimized Scheme)	Change
Maximum Displacement (mm)	31.2	14.7	↓52.88%
Average Displacement (mm)	20.8	10.9	↓47.60%
Safety Factor Fs	1.08	1.46	↑35.19%
Maximum Shear Strain	0.018	0.009	↓50.00%
Displacement Control Rate η	—	52.88%	—
Number of Iterations for Convergence	78	64	↓17.95%

As shown in Table 3, after reinforcement and optimization, the overall mechanical response of the slope was significantly improved, and all key indicators showed favorable changes. Firstly, in terms of deformation control, the maximum displacement decreased from 31.2 mm to 14.7 mm, a reduction of 52.88%, and the average displacement decreased by 47.60%, indicating that the optimized reinforcement scheme can effectively suppress the overall and local deformation of the slope and significantly improve the structural stiffness and stability. Secondly, in terms of stability indicators, the safety factor increased from 1.08 to 1.46, an increase of 35.19%, indicating that the slope changed from a near-critical state to a stable state that meets the specifications, with a significantly enhanced safety reserve.

5. Conclusion

This paper addresses the problems of parameter uncertainty and insufficient reinforcement design optimization in the stability analysis of rock slopes, and proposes an integrated method for displacement back analysis and reinforcement optimization based on intelligent computing. By constructing a parameter back-analysis model constrained by measured displacement and combining it with an intelligent optimization algorithm, high-precision identification of key mechanical parameters of the rock mass was achieved. Based on this, a numerical calculation model driven by inversion parameters is established to perform coupled analysis of slope displacement response and stability, and to effectively identify potential slip modes through deformation feature extraction. Furthermore, a multi-objective reinforcement optimization model is constructed to inversely calculate and optimize key parameters such as anchor bolts. It should be noted that this study is mainly based on a two-dimensional numerical model and typical working conditions, and has not fully considered the influence of complex three-dimensional geological structures and multi-field coupling on slope response. Future research can further combine three-dimensional fine modeling with multi-source monitoring data fusion methods, and introduce advanced intelligent algorithms such as deep learning to improve the model's generalization ability and engineering

applicability, achieving a higher level of intelligent development in rock slope stability analysis and reinforcement design.

Acknowledgement

This work was supported by Luzhou city Science and Technology Bureau(2025MYF048).

References

[1] Zheng H, Wu X, Jiang Y, et al. Shear behavior of rock joints reinforced with fully-grouted and energy-absorbing bolts subjected to shear cycles[J]. Journal of Rock Mechanics and Geotechnical Engineering, 2025, 17(7): 4314-4328.
[2] Zhang N, Zou S, Mao Z, et al. The Influence of the Reinforcement Method of Anti-slide Piles on Slope Stability[J]. ce/papers, 2025, 8(2): 703-709.
[3] Li H, Zhang B, Wang L, et al. Numerical Analysis and Reinforcement Study of a Roadside Slope in Xinjiang[J]. Advances in Engineering Technology Research, 2025, 14(1): 35.
[4] Kuo H L, Lin G W, Lin T Y, et al. Displacement evolution of failure and non-failure sliding rock slopes[J]. Landslides, 2025, 22(4): 1213-1226.
[5] Amagu C A, Zhang C, Kodama J, et al. 3-D numerical analysis of mining-induced deformation of clay-bearing rock slope in a quarry[J]. Rock Mechanics and Rock Engineering, 2025, 58(6): 6145-6167.
[6] Zhang J, Huang D, Li Z, et al. Step-path failure of the rock slopes with large intersection angles between the strikes of strata and surface: a case study[J]. Journal of Mountain Science, 2025, 22(3): 931-949.
[7] Zhao Q, Yang Z, Zhang S, et al. Exploring the toppling deformation mechanisms and failure modes of anti-dip layered rocky slopes: insights from physical model experiments[J]. Landslides, 2025, 22(3): 895-923.
[8] Tao Z, Xie G, Liu Y, et al. Investigation of high rock slope failure mechanisms: a case study of a uranium mine in Namibia[J]. Journal of Mountain Science, 2025, 22(4): 1446-1461.
[9] Maheshwari S, Bhowmik R, Cuomo S. Impact performance of unreinforced and geogrid-reinforced rockfall protection embankment[J]. Geosynthetics International, 2025, 32(3): 321-341.